Distribution and binding of ^{18}F-labeled and ^{125}I-labeled analogues of ACI-80, a prospective molecular imaging biomarker of disease: A whole hemisphere post mortem autoradiography study in human brains obtained from Alzheimer's disease patients

Balázs Gulyás [a,*], Christian Spenger [b,c], Zsuzsa Beliczai [d], Károly Gulya [d], Péter Kása [e], Mahabuba Jahan [a], Zhisheng Jia [a], Urs Weber [f], Andrea Pfeifer [f], Andreas Muhs [f], Dieter Willbold [g,h], Christer Halldin [a]

[a] Karolinska Institutet, Department of Clinical Neuroscience, Psychiatry Section, S-171 76 Stockholm, Sweden
[b] Karolinska Institutet, Department of Clinical Science, Intervention and Technology, S-141 83 Stockholm, Sweden
[c] Prodema Medical AG, CH-9552 Bronschhofen, Switzerland
[d] Department of Cell Biology and Molecular Medicine, University of Szeged, H-6720 Szeged, Hungary
[e] Department of Psychiatry, University of Szeged, H-6720 Szeged, Hungary
[f] AC Immune, PSE Building B, EPFL, CH-1015 Lausanne, Switzerland
[g] Forschungszentrum Jülich, Institut für Strukturbiologie und Biophysik (ISB-3), D-52425 Jülich, Germany
[h] Heinrich-Heine-Universität, Institut für Physikalische Biologie, D-40225 Düsseldorf, Germany

ARTICLE INFO

ABSTRACT

One of the major pathological landmarks of Alzheimer's disease and other neurodegenerative diseases is the presence of amyloid deposits in the brain. The early non-invasive visualization of amyloid is a major objective of recent diagnostic neuroimaging approaches, including positron emission tomography (PET), with an eye on follow-up of disease progression and/or therapy efficacy. The development of molecular imaging biomarkers with binding affinity to amyloid in the brain is therefore in the forefront of imaging biomarker and radiochemistry research. Recently, a dodecamer peptide (amino acid sequence = QSHYR-HISPAQV; denominated D1 or ACI-80) was identified as a prospective ligand candidate, binding with high *ex vivo* affinity to L-Aβ-amyloid (K_d: 0.4 μM). In order to assess the ligand's capacity to visualize amyloid in Alzheimer's disease (AD), two ^{125}I labeled and three ^{18}F labeled analogues of the peptide were synthesized and tested in post mortem human autoradiography experiments using whole hemisphere brain slices obtained from deceased AD patients and age matched control subjects. The ^{18}F-labeled radioligands showed more promising visualization capacity of amyloid that the ^{125}I-labeled radioligands. In the case of each ^{18}F radioligands the grey matter uptake in the AD brains was significantly higher than that in control brains. Furthermore, the grey matter: white matter uptake ratio was over ~2, the difference being significant for each ^{18}F-radioligands. The regional distribution of the uptake of the various radioligands systematically shows a congruent pattern between the high uptake regions and spots in the autoradiographic images and the disease specific signals obtained in adjacent or identical brain slices labeled with histological, immunohistochemical or autoradiographic stains for amyloid deposits or activated astrocytes. The present data, using post mortem human brain autoradiography in whole hemisphere human brains obtained from deceased AD patients and age matched control subjects, support the visualization capacity of the radiolabeled ACI-80 analogues of amyloid deposits in the human brain. Further studies are warranted to explore the usefulness of the ^{18}F-labeled analogues as *in vivo* molecular imaging biomarkers in diagnostic PET studies.

© 2011 Elsevier Ltd. All rights reserved.

1. Introduction

Alzheimer's disease (AD) is a debilitating neurodegenerative disorder for which no therapies are available that can halt or delay the disease process. A number of potential drugs, however, are under investigation in early clinical phases and it therefore

becomes important that methods for the early detection of the disease are developed in parallel. AD has especially great importance for the society as with increased life expectancy world-wide the proportion of AD patients is increasing. For example the number of AD patients between 2006 and 2050 is expected to quadruple (Brookmeyer et al., 2007, 2011). This causes heavy challenges to the health care and social system in particular since approximately 40% of the prevalent cases need intense level of care. Despite intensive research efforts in the past decades, the reliable diagnosis of AD is still based on the post mortem demonstration of amyloid plaques and neurofibrillary tangles in the diseased person's brain. A reliable early *in vivo* clinical diagnostic approach would be a unique asset, but is still seriously hampered by the lack of diagnostic probes with sufficient sensitivity and specificity.

With the help of molecular imaging techniques, including positron emission tomography (PET), molecular alterations, underlying pathological conditions leading to brain diseases, can be recognized distinctively in its early phase. Consequently, they have a unique potential to identify very early molecular dysfunctions that are predictive for the imminent or future development of AD, they are useful for early diagnosis, prognosis prediction, refined diagnostic classification, and quantification and follow-up of drug treatment efficacy. In line with this potential of molecular imaging techniques, especially PET, the search for molecular imaging biomarkers as diagnostic probes for PET investigations in the early phase of AD has been intensified during the past years (Rabinovici and Jagust, 2009; Cavedo and Frisoni, 2011; Prvulovic and Hampel, 2011; Scheinin et al., 2011; Galimberti and Scarpini, 2011).

Amyloid and insoluble Aβ peptides have been identified as disease biomarkers (Andreasen and Zetterberg, 2008; Hampel et al., 2008; Svedberg et al., 2009; Lin et al., 2010a,b) for which molecular imaging biomarkers have also been developed (Klunk et al., 2004; Nordberg, 2007, 2008; Cai et al., 2007). Activated microglia and the up-regulated peripheral benzodiazepine (PBR) or, as it is recently called, 18 kDa translocator protein (TSPO) system (Banati, 2002; Venneti et al., 2006; Chen and Guilarte, 2008; Gavish et al., 1999; Gulyás et al., 2002a,b, 2009, 2011a,b) are other evident candidates, as are, among others, β-adrenergic receptors (Wang et al., 2011; Yu et al., 2011), activated astrocytes and the MAO-B system (Schwab and McGeer, 2008; Fuller et al., 2009; Rodríguez et al., 2009; Razifar et al., 2006; Johansson et al., 2007; Gulyás et al., 2011a,b,c; Nag et al., 2011). For the latter targets, molecular imaging biomarkers are already available (Fowler et al., 1995; Kumlien et al., 1995; Reutens, 2000; Kassiou et al., 2005; Dollé et al., 2009; Gulyás et al., 2011a,b,c). Other targets, including cardinal neurotransmitter receptors and transporters, neuromodulatory and neuroregulatory proteins, have also been considered.

During the search for an appropriate molecular imaging biomarker for amyloid, a dodekamer peptide (amino acid sequence = QSHYRHISPAQV; denominated D1 or ACI-80) was identified as a prospective ligand binding with high ex vivo affinity to L-Aβ-amyloid (K_d: 0.4 μM) (Schumacher et al., 1996; Wiesehan et al., 2003; Wiesehan and Willbold, 2003). More recently, the molecule's potential for reducing plaque load in transgenic (tg) mice by one of its analogues (van Groen et al., 2008, 2009) and the inhibition of cell toxicity and neurofibrillary tangle formation by ACI-80 were also demonstrated (Wiesehan et al., 2008), indicating the compound's therapeutic property, in addition to its diagnostic potential.

In order to demonstrate the affinity of ACI-80 to amyloid plaques in the human brain in AD and with an eye on using the compound in *in vivo* imaging studies as a molecular imaging biomarker for AD, we have performed *ex vivo* experiments using [¹⁸F]-radiolabeled and [¹²⁵I]-labeled analogues of the compound.

The studies included whole hemisphere autoradiographic experiment on brain slices obtained from both AD patients and age matched controls. In order to demonstrate the presence of amyloid plaques in the AD brain tissue and the congruence between the autoradiographic signal and the presence of amyloid plaques, immunohistochemical studies were performed in the same brains.

2. Methods

2.1. Radiochemistry

2.1.1. Synthesis of [¹²⁵I]-compounds ([¹²⁵I]ACI-80 and [¹²⁵I]ACI-80-F)

The peptides to be labeled (D1 or ACI-80 and ACI-80-F) were received from the Forschungszentrum Jülich, Germany. Chloramide-T was obtained from Aldrich, potassium iodide and PBS (pH 7.0) from Fluka, Iodide-125 (10 mCi/100 μl) from PerkinElmer. Peptide monoiodides were analysed and purified by HPLC (Merck Hitachi), equipped with UV detector and radiodetector (Packard). A semi-preparative reverse phase column (Waters μ-Bondapak C18, 10 m, 8.7 × 300 mm) was used with a UV detector set at 22 nm. The reaction mixture comprised 10 μl Na ¹²⁵I (1 mCi), 100 μl peptide, 1 mg/ml EtOH in water (1/1, v/v), 300 μl BPS (pH 7.0), 100 μl chloramine-T (3 mg/2 ml water). The reaction mixture stood at room temperature for 1–2 min and then was loaded into the HPLC column, eluted with mobile phase trifluoroacetic acid (0.1%, v/v): MeOH (72/28, v/v) at flow rate 3 ml/min. The solvent from the collected fraction was removed by evaporator below 40 °C under vacuum afforded the respective peptide iodide, which was then formulated with 50% ethanol in water. The analysis of the peptide monoiodides was performed in the same HPLC system and its identification was made by an LC–MS system (Waters Q-Tof Premier mass spectrometer system with Acquity UPLC). Radiochemical purity was more than 98%. The investigated ᴅ-enantiomeric peptide compounds are listed in Table 1 and the radiolabeled peptides' structures are shown in Fig. 1.

2.1.2. Synthesis of [¹⁸F]-compounds ([¹⁸F]ACI-87-F, [¹⁸F]ACI-88-F, [¹⁸F]ACI-89-F)

The variants of ACI-80, labeled with [¹⁸F], were designed for increased stability in water and increased binding strength compared to ACI-80 (cfr. Table 1). N-succinimidyl-4-[¹⁸F]fluorobenzoate ([¹⁸F]SFB) was synthesized based on the literature method with modifications (Tang et al., 2008; Johnström et al., 2008). To a solution of [¹⁸F]-SFB (200 μl – 900 MBq) in acetonitrile, peptide (1.2 mg) in borate buffer (150 μl, pH = 8.8) was added and kept at room temperature (RT) for 10 minutes. The reaction mixture was then injected into C18 μBondapak reverse phase analytical HPLC column (3.9 × 300 mm, 10 μm, Waters) using a gradient method MeCN-0.1% TFA (20% of MeCN to 50% MeCN) as eluent with flow rate of 2 ml/min. The effluent was monitored with UV absorbance detector (λ = 224 nm) in series with a GM tube

Table 1
List of investigated ᴅ-enantiomeric peptide compounds. Modifications in the original amino acid sequence of ACI-80 are printed in bold. Other modifications of the amino acid sequence are printed in italics. FITC: fluorescein isothiocyanate.

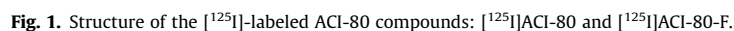| Name of compound	Amino acid sequence	Modification
[¹²⁵I]-ACI-80	QSHYRHISPAQV-(¹²⁵I)	D1-[¹²⁵I]
[¹²⁵I]-ACI-80-F	QSHYRHISPAQV-(¹²⁵I)-FITC	D1-FITC
[¹⁸F]-ACI-87-F	QSHYRHISPAQ**K**-(¹⁸F)-FITC	D1-V12K-[¹⁹F]-FITC
[¹⁸F]-ACI-88-F	SHYRHISPAQ**K**-(¹⁸F)-FITC	Q1X-D1-V12 K-[¹⁹F]-FITC
[¹⁸F]-ACI-89-F	**P**SHYRHISPAQ**K**-(¹⁸F)-FITC	D1-Q1P-V12 K-[¹⁹F]-FITC

Fig. 1. Structure of the [125I]-labeled ACI-80 compounds: [125I]ACI-80 and [125I]ACI-80-F.
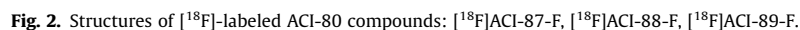

Fig. 2. Structures of [18F]-labeled ACI-80 compounds: [18F]ACI-87-F, [18F]ACI-88-F, [18F]ACI-89-F.

radioactivity detector. The product fraction [18F]-peptides, was collected (R_t = 10–12 min) in a pre-filled slightly basic (pH was adjusted with NaOH) aqueous solution (40 ml). This diluted product fraction was then passed through a C18 Sep-Pak plus cartridge (preconditioned with 10 ml EtOH + 10 ml water) and the desired product, ([18F]ACI-87-F, [18F]ACI-88-F, [18F]ACI-89-F), was eluted with 1 ml of ethanol. The identity of these radiotracers ([18F]-peptides) were confirmed using HPLC by co-injecting with an unlabeled reference of [19F]-peptides. The radiotracers were formulated in phosphate buffered saline (PBS; pH = 7.4; 7 ml) and filtered through a sterile filter (0.22 μm; Millipore, Sweden) into a sterile vial for *in vivo* applications. Total time of synthesis was 40 min from the end of synthesis of [18F]-SFB. The radiochemical purity of [18F]-peptides were >98% and the obtained specific

radioactivity values were for [18F]ACI-87-F 16 GBq/μmol and 11 GBq/μmol, for [18F]ACI-88-F 113 GBq/μmol and 9 GBq/μmol, and for [18F]ACI-89-F 86 GBq/μmol and 27 GBq/μmol. The investigated ᴅ-enantiomeric peptide compounds are listed in Table 1 and the radiolabeled peptides' structures are shown in Fig. 2.

2.1.3. Synthesis of reference peptides

To an aqueous solution of peptide, borate buffer (0.5 M, pH = 8.61) was added and the color of the solution changed from yellow to dark orange. Slightly excess amount of SFB in acetonitrile was added into this above solution and the reaction mixture was kept at RT for 10 min. The reaction was monitored by HPLC. The crude product was purified by an analytical HPLC column (3.9 × 300 mm, 10 μm, Waters, Milford, MA) using a gradient

method MeCN-0.1% TFA (20% of MeCN to 50% MeCN) as eluent with flow rate of 2 ml/min. Retention times for the three reference peptides were from 9 to 12 min and the wavelength was $\lambda = 234$ nm. The product fraction was then collected into a pre-filled slightly basic aqueous solution (40 ml, pH was adjusted by NaOH). This diluted fraction was passed through a C18 Sep-Pak plus cartridge (preconditioned with 10 ml EtOH + 10 ml water) and the desired product was eluted with 1 ml of ethanol. The reference compounds were confirmed by LC–MS/MS. The purity and the stability of the products were analyzed by HPLC.

2.1.4. Synthesis of [11C]-L-deprenyl

The MAO-B imaging radiotracer [11C]-L-deprenyl was labeled as described earlier (Gulyás et al., 2011a,b,c).

2.2. Brain tissue

Fresh frozen whole hemisphere brain slices of human brains were received from the Alzheimer Research Group of the Albert Szent-Györgyi Medical and Health Science Center, University of Szeged, Hungary. The samples used for the present and consequent studies included brains from 4 Alzheimer's patients and 5 age-matched control subjects whereof only a selected sample size is referred to in the present investigation. Ethical permission was obtained from the Research Ethics Committee of the University of Szeged (1895/2004, Hungary). The post mortem time interval was between 2.5 h and 5.0 h. The patients' age was between 50 and 98 years, and the collection of AD brains covered Braak stages between I/II–V. The brains had been removed during clinical autopsy and were handled in a manner similar to that described previously (Hall et al., 1998; Varnäs et al., 2004; Gulyás et al., 2009, 2010, 2011). The sectioning of the brains and all further autoradiographic procedures were performed at the Department of Clinical Neuroscience, Karolinska Institutet, Stockholm, Sweden. Coronal brain slices of 100 μm thickness were made in a Leika cryomacrocut system. Ethical permission for the autoradiographic experiments were obtained from the Regional Research Ethics Committee of North Stockholm, Sweden (2010/372-32).

2.3. Autoradiography

2.3.1. 125I compounds ([125I]ACI-80 and [125I]ACI-80-F)

[125I]ACI-80 and [125I]ACI-80-F ARG was performed on 100 μm thick coronal slices of whole human hemispheres obtained from two Alzheimer's patients: a 50 year old female (Braak stage II–III) and a 96 year old female (Braak stage V). The incubation buffer consisted of 50 mM Tris–HCl containing the salts NaCl, KCl, CaCl$_2$, MgCl$_2$, as well as 0.01% ascorbic acid and 0.01% bovine serum albumine, pH 7.4. Further to preliminary experiments on human brain slices with a series of increasing radioligand concentrations, an optimal concentration was determined and in the present experiments the incubation solution contained the radioligand in 4.0 nM concentration. The rinsing buffer contained 50 mM Tris–HCl (no salt) with pH 7.4. The incubation was done for 60 min at room temperature (RT). Rinsing was then performed twice for 5 min at 4 °C with rinsing buffer (see above) at RT; followed by dipping in ice cold distilled water. The slides were then placed on an imaging plate (Fujifilm Plate BAS-TR2025, Fujifilm, Tokyo, Japan) for 22–24 h. The plates were developed and the resulting images were processed in a Fujifilm BAS-5000 phosphorimager (Fujifilm, Tokyo, Japan). Aliquots (20 μl) of the incubation solution were spotted onto polyethylene-backed absorbent paper (BenchGuard™), allowed to dry, scanned and digitized in the phosphorimager parallel with the tissue scans. The ARG signal's optical density (OD) was measured, using Multi Gauge 3.2 image analysis software (Fujifilm, Tokyo, Japan). Using the known radioactivity value of the aliquots and the OD values, we could also quantify the radioligand uptake values in various brain structures in nM/g units.

2.3.2. 18F compounds (ACI-87-F, ACI-88-F, ACI-89-F)

Using [18F]-labeled ACI-87-F, ACI-88-F, ACI-89-F ARG was performed on fresh frozen whole hemisphere brain slices of human brains obtained from both AD patients and aged matched control subject.

The ARG was performed on fresh frozen whole hemisphere brain slices. The measurements were done in duplicates. Incubation of [18F]ACI-87-F, [18F]ACI-88-F and [18F]ACI-89-F was prepared at radioligand concentration of 0.02 MBq/ml for 90 min, at room temperature (RT). The incubation buffer consisted of 50 mM Tris-HCl containing the salts NaCl, KCl, CaCl$_2$, MgCl$_2$, as well as 10 μM pargylin and 0.3% bovine serum albumine, pH 7.4. The rinsing buffer contained 50 mM TRIS HCl (no salt), the pH was 7.4. Rinsing was then performed three times for 5 min at 4 °C with rinsing buffer; followed by dipping in ice cold distilled water.

The exposed brain slices were placed on an image plate (Fujifilm Plate BAS-TR2025, Fujifilm, Tokyo, Japan) for at least 120 min. The readings were made and digitized in a Fujifilm BAS-5000 phosphorimager (Fujifilm, Tokyo, Japan).

Aliquots (20 μl) of the incubation solution (0.02 MBq/ml) and the diluted incubation solution (50% incubation solution: 50% TRIS buffer; 0.01 MBq/ml) were spotted onto polyethylene-backed absorbent paper (BenchGuard), allowed to dry, scanned and digitized in the phosphorimager parallel with the tissue scans.

The ARG signal was quantified using Multi Gauge 3.2 image analysis software (Fujifilm, Tokyo, Japan). The average ratios (five measurements per structure per brain) of grey matter-white matter uptake, expressed in radioactivity uptake (Bq/g; the gram-value represents "dry" tissue weight throughout the paper) of the three [18F]-D-peptides ([18F]ACI-87-F, [18F]ACI-88-F and [18F]ACI-89-F) in the Alzheimer's disease and age matched control brain slices were calculated. Using the known radioactivity value of the aliquots and the OD values, we could also quantify the radioligand's radioactivity uptake values in various brain structures in Bq/g units.

2.3.3. [11C]deprenyl autoradiography

In order to have a "reference measurement", by using [11C]deprenyl as an established radioligand labeling activated astrocytes in neuroinflammation, ARG was performed on fresh frozen whole hemisphere brain slices of human brains from both AD patients and aged matched control subject as reference for the localization of activated astrocytes in the brain slices. The procedures were identical with those described by Gulyás et al. (2011).

2.4. Histology and immunohistochemistry: human brain

2.4.1. Amyloid staining with Congo red

Fresh frozen brain slices of 100 μm thickness were fixed in 0.1 M TBS (Tris-buffered saline; pH 7.5) containing 4% formaldehyde for 10 min and washed for 3 × 5 min in 0.1 M TBS in RT. Tissue autofluorescence was inhibited by staining the sections with Mayer hematoxylin solution (100 mg hematoxylin, 20 mg Na-iodate, 5 g aluminum potassium sulfate, 5 g trichloroacet-aldehyde nitrate and 100 mg citric acid dissolved in 100 ml) for 2 min, washed for 5 min in tap water, and rinsed for a few seconds in distilled water (all in RT). The sections were then incubated in an ethanolic saturated NaCl solution (50 ml of a saturated NaCl solution (30 g NaCl, 200 ml distilled water, 800 ml 100% ethanol) and 0.5 ml 1% NaOH) for 30 min at 60 °C. The sections were then transferred to a Congo red solution (1:1 solution A:solution B; solution A: 1 g Congo red, 1 g sodium carbonate, 100 ml distilled water; solution B: 50 ml distilled water, 50 ml 100% ethanol) and

incubated for 30 min at 60 °C. The sections were then rinsed in distilled water and covered in a mixture (1:1) of glycerine/distilled water and coverslipped.

2.4.2. Astrocyte staining with GFAP immunohistochemistry (DAB)

The cryostat sections were fixed in 0.5 M PBS (phosphate-buffered saline; pH 7.5) containing 4% formaldehyde for 10 min and washed for 3×5 min in 0.05 M PBS in room temperature (RT). After blocking the endogenous peroxidases in 1% H_2O_2 for 30 min in 37 °C, the sections were washed for 3×5 min in 0.05 M PBS. The tissue sections were permeabilized and the background binding of the antibodies were reduced in a blocking solution (0.05 M PBS solution containing 3% NGS, 1% BSA, 0.05% Triton X-100) for 60 min at 37 °C. Sections were then covered with a solution containing mouse anti GFAP primary antibody (diluted to 1:500 in the blocking solution) at 4 °C overnight, then washed for 4×10 min in 0.05 M PBS in RT. The sections were treated with a biotinylated anti mouse IgG secondary antibody diluted (1:200) in the blocking solution (where Triton X-100 was omitted) for 6 h at RT. After several washes (4×10 min), biotinylated streptavidin-peroxidase tertiary antibody (1:200) in the blocking solution (without Triton X-100) overnight at 4 °C.

The sections were washed again in 0.05 M PBS for 4×10 min at RT and processed for peroxidase enzyme histochemistry. The sections were pre-incubated in a filtered 0.05 M PBS solution containing 0.5 mg/ml DAB for 20 min at RT, and then developed in the same solution but also containing 0.01% H_2O_2 for 10–20 min at RT. The sections were finally washed for 3×5 min in 0.05 M PBS, mounted on glass slides, dehydrated in a series of alcohol solutions, covered with DPX and coverslipped.

3. Results

3.1. [^{125}I]-labeled compounds

Autoradiographic images, together with characteristic immunohistochemical images, from the two AD brains are displayed in Fig. 3. At visual inspection and at microscopic investigation, both brains showed clear signs of degeneration and atrophy compatible with the disease. Artifacts due to the acquisition and conservation of the tissue were also seen. Congo red stain, performed on adjacent sections showed intense diffuse staining throughout the sections in both patients' brain, together with abundant Congo red positive plaques. GFAP staining of the brains indicated extensive and clear-cut astrocyte activation in the tissue.

[^{125}I]-ACI-80 ARG of both brains displayed very distinct cortical and sub-cortical labels in form of distinct spots and a diffuse label of the cortical areas including the hippocampus. The ARG signal in brain of the older patient with higher Braak-grade (Braak stage V) was clearly stronger than that in the brain of the younger patient with lower Braak-grade (Braak II–III), compatible with an increased plaque load in the former. For [^{125}I]ACI-80-F a similar, though more diffuse labeling pattern was seen in both brains as compared to the pattern obtained with [^{125}I]ACI-80. The average (± standard error of means, SEM) uptake of [^{125}I]-ACI-80 in the cortical grey matter was 0.478 ± 0.020 nM/g, and for the white matter it was 0.396 ± 0.017 nM/g, and for the hippocampus it was 0.457 ± 0.020 nM/g (n.s.). The grey matter:white matter ratio was 1.21 ($p = 0.0002$), the hippocampus:white matter ratio was 1.15 ($p = 0.0369$). The average uptake of [^{125}I]-ACI-80-F in the cortical grey matter was 0.435 ± 0.016 nM/g, for the white matter it was 0.407 ± 0.019
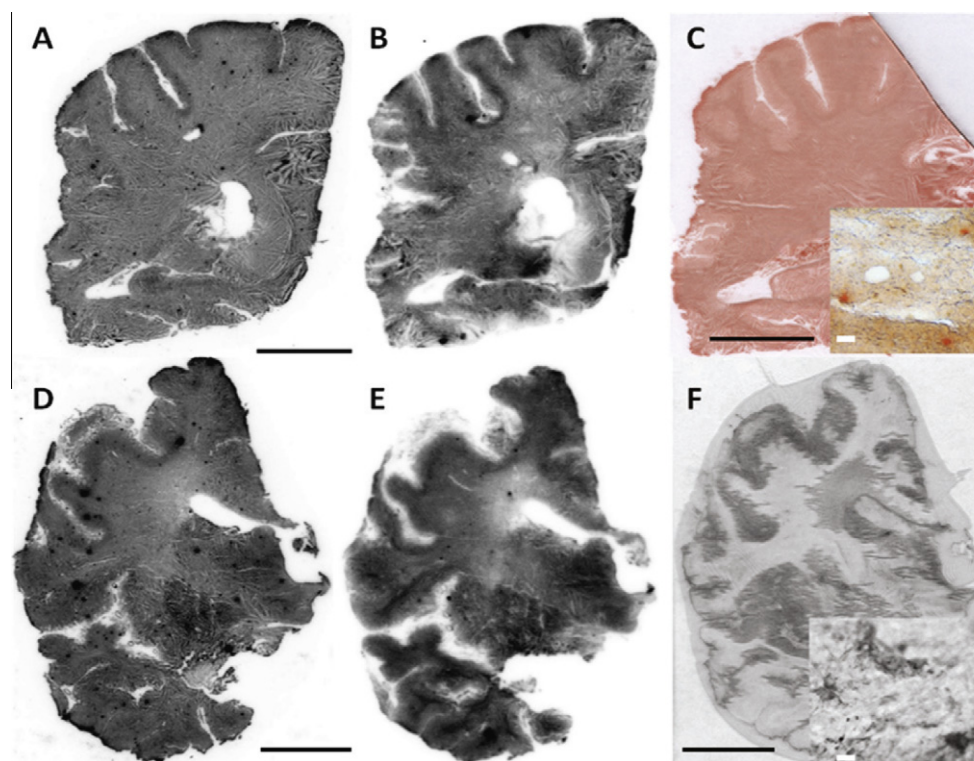

Fig. 3. Autoradiography, histochemistry and immunohistochemistry results obtained in whole hemisphere sections of two AD brains. A–C: Brains slices obtained from a 50 year old female AD patient, Braak II–III; D–F: Brains slices obtained from a 96 year old female AD patient, Braak V. A and D: autoradiograms obtained with [^{125}I]-ACI-80. B and E: autoradiograms obtained with [^{125}I]-ACI-80-F. C: Congo red stain demonstrating amyloid deposition in the brain. In the zoomed-up panel red-orange plaques indicate amyloid deposits. F: GFAP immunohistochemistry, displaying activated astrocyes. In the zoomed-up panel the cells stained in dark-grey are activated astrocytes. Scale bars in black (A, B, D and E): 20 mm, scale bars in white (C and F): 50 µm.
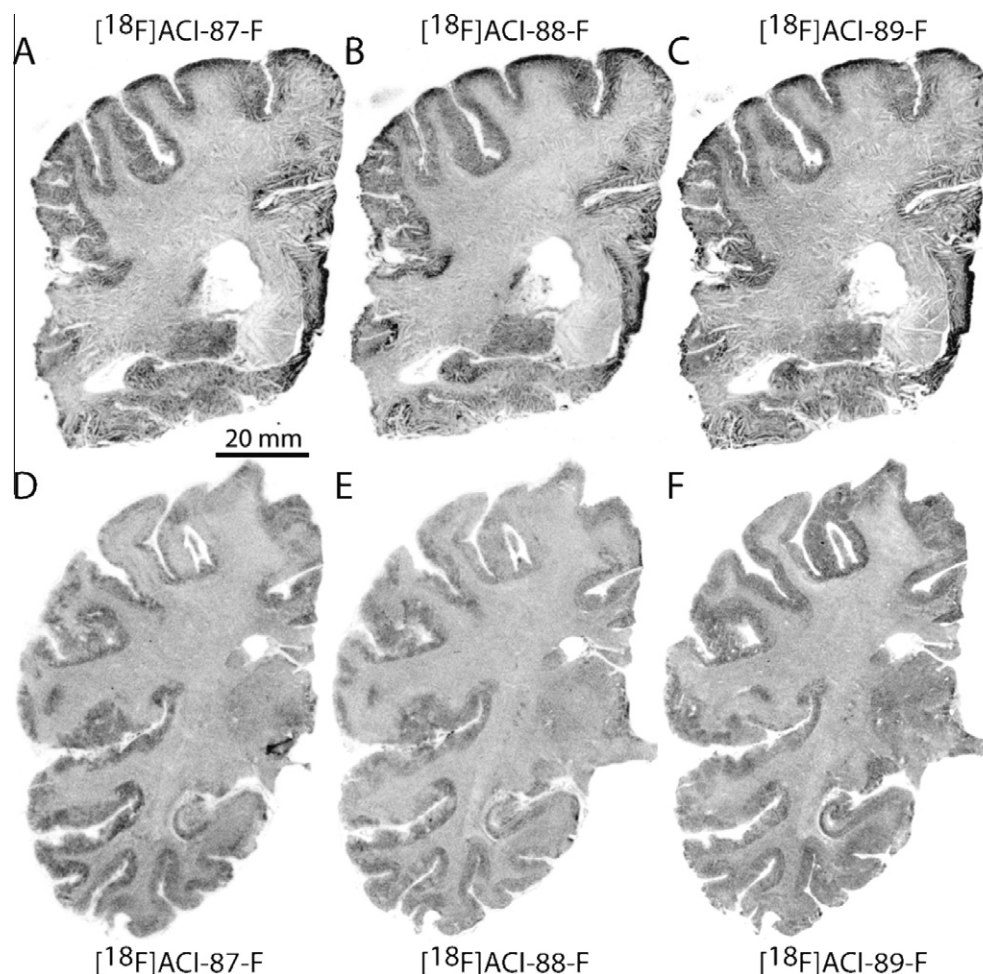
Fig. 4. [^{18}F] ACI-87F, [^{18}F] ACI-88F and [^{18}F] ACI-89F autoradiography in an Alzheimer's and a control brain. Autoradiographs of human brain hemispheres demonstrating total [^{18}F]ACI-87-F, [^{18}F]ACI-88-F and, [^{18}F]ACI-89-F binding in coronal sections at the level of hippocampus. The brain slices were obtained form a 50 year old female with AD (A–C) and an age matched control subject (50 years female, D–F).

nM/g, and for the hippocampus it was 0.425 ± 0.019 nM/g. The grey matter:white matter ratio was 1.07 (n.s.), the hippocampus:white matter ratio was 1.04 (n.s.).

3.2. [^{18}F]-labeled compounds

ARG with [^{18}F]ACI-87-F, [^{18}F]ACI-88-F, and [^{18}F]ACI-89-F was performed in coronal brain slices of a 50 year old female with AD (Braak II–III – same brain as used for [^{125}I] ARG shown in Fig. 2) and on coronal slices of an aged matched control patient (54 years, female).

As can be seen in Fig. 4, [^{18}F]ACI-87F, [^{18}F]ACI-88F and [^{18}F]ACI-89F ARG showed a diffuse signal in the cortical layers and ventral and dorsal hippocampal formation in the AD patients. The radioligand uptake values in the cortical grey matter, the white matter and in the hippocampus, as well as the grey matter:white matter and hippocampus:white matter ratios for the three radioligands in the diseased and control brains are shown in Table 2, the corresponding significance values are displayed in Table 3. The signal was distinctively stronger in AD brains that in the brains obtained from age matched control subjects. Also, while in the control subjects' brain the layers of the hippocampal formation are visible, the ARG signal in the hippocampus of the AD patient was diffuse, more intense and there were no layers visible. Moreover, some very

strong labeled spots in the cortical areas and hippocampus of the Alzheimer's patient were visible for all there radioligands: [^{18}F]ACI-87-F, [^{18}F]ACI-88-F and [^{18}F]ACI-89-F. This was practically absent in the slices of the control brain.

As shown in the table and in the images, the signal in the cortex and hippocampus was more intense in the case of AD brains as compared to the age matched control brains.

Table 2
Radioligand uptake values for the three ligands ([^{18}F] ACI-87-F, [^{18}F] ACI-88-F and [^{18}F] ACI-89-F) in an Alzheimer's and a control brain and their ratios. The levels of significance of the differences are shown in Table 3 (Student's t-test, one tailed, unequal variance). Values are expressed in radioactivity uptake in the brain tissue (average ± SEM; Bq/g. Values were obtained from five ROI's (region-of-interest) in each slice. G: grey matter, W: white matter.

		[^{18}F]ACI-87-F	[^{18}F]ACI-88-F	[^{18}F]ACI-89-F
Control	G	4.15 ± 0.10	4.95 ± 0.18	5.08 ± 0.14
	W	2.72 ± 0.06	3.53 ± 0.08	4.00 ± 0.08
	G/W ratio	1.53	1.40	1.27
AD	G	4.98 ± 0.26	6.46 ± 0.35	7.57 ± 0.27
	W	2.28 ± 0.10	3.12 ± 0.16	4.23 ± 0.27
	G/W ratio	2.18	2.07	1.79
AD: control	G:G	1.20	1.31	1.49
	W:W	0.84	0.88	1.06

Table 3
Levels of significant differences between parametric values shown in Tables (Student's *t*-test, one tailed, unequal variance). G: grey matter, W: white matter, Ctrl: control, vs: versus.

		[^{18}F]ACI-87-F	[^{18}F]ACI-88-F	[^{18}F]ACI-89-F
G vs W	Ctrl	***	***	***
	AD	***	***	***
Ctrl vs AD	G	***	***	***
	W	**	*	n.s.
		[^{18}F]ACI-87-F vs. [^{18}F]ACI-88-F	[^{18}F]ACI-87-F vs. [^{18}F]ACI-89-F	[^{18}F]ACI-88-F vs. [^{18}F]ACI-89-F
G vs G	Ctrl	**	***	n.s.
	AD	**	***	*
W vs W	Ctrl	***	***	***
	AD	**	***	n.s.

n.s., not significant.
* $p < 0.05$.
** $p < 0.01$.
*** $p < 0.001$.

3.3. Comparing autoradiographic brain uptake patterns with [^{18}F]-labeled compounds and with [^{11}C]-L-deprenyl

In addition to labeling amyloid deposits in the brain, complimentary ARG was performed using [^{11}C]-L-deprenyl, an established molecular imaging biomarker of activated astrocytes and the MAO-B system, in order to visualize astrocyte activation and the upregulation of MAO-B, as a sign of neuroinflammation, concurrent with amyloid deposits in AD. As shown in Fig. 5, the spotty up-take pattern, observed in the cortex of the brain of AD patients with the radioflurinated ACI peptides, was also seen with [^{11}C]-L-deprenyl, although due to the different energy ranges of ^{11}C and ^{18}F the up-take pattern was more blurred. This may indicate a concurrent neuroinflammation, resulting in the up-regulation of astrocytes, in the very same regions where the higher regional up-take of the radioflurinated ACI peptides indicates amyloid depositions.

3.4. Comparison of autoradiography and histochemichal and immunohistochemical data

In order to visualize the pattern of regional amyloid depositions in the brain and compare this with the ARG findings, we performed histochemical amyloid staining with Congo red in brain slices,
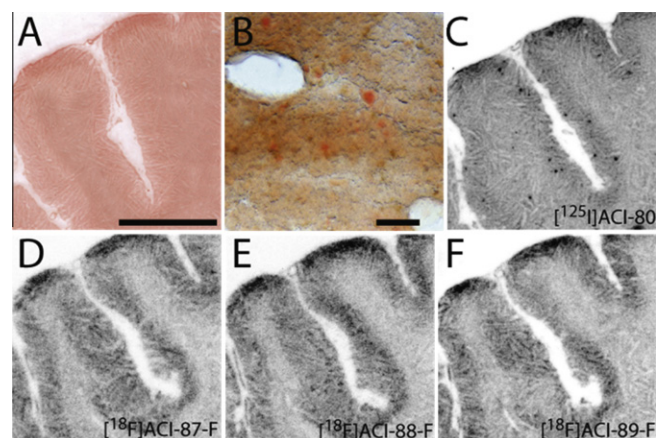

Fig. 6. Histochemical staining with Congo red (panels A and B) and autoradiography (panels C–F) obtained from adjacent brain slices (100 μm thickness) from the same AD patient (50 years old female, Braak stage II–III). Magnifications in panels A and C–F are identical and the scale bar indicates 1 cm. The scale bars in B is 100 μm. The radioligands were [^{125}I]ACI-80 (C), [^{18}F]ACI-87-F (D), [^{18}F]ACI-88-F (E) and [^{18}F]ACI-89-F (F).

adjacent to those whereon ARG was made. As shown in Fig. 6A, a diffuse labeling of the tissue was seen with Congo red. High magnification Fig. 6B of the cortical area shows numerous plaques as indicated by Congo red spots in the photomicrographs. The Congo red spots are of different size and intensity, indicating both diffuse and more circumscribed amyloid deposition pattern in the brain of AD patients. Panels C–F display ARG images of the same sulcus which is present in panel A. The ARG staining in Fig. 6C was made with [^{125}I]ACI-80, whereas in Fig. 6D and F they were made with three radiofluorinated compounds. Despite the fact that the ARG signals show varying intensities depending upon the radionuclide ([^{18}F] or [^{125}I]) and the compound (ACI-80, ACI-87-F, ACI-88-F, ACI-89-F), in overall, the immunohistochemical signals are congruent with the ARG signals, indicating increased amyloid deposition in the cortex of AD brains.

4. Discussion

The advent of molecular imaging techniques, with special regard to PET, has revolutionized diagnostic medicine as the use of
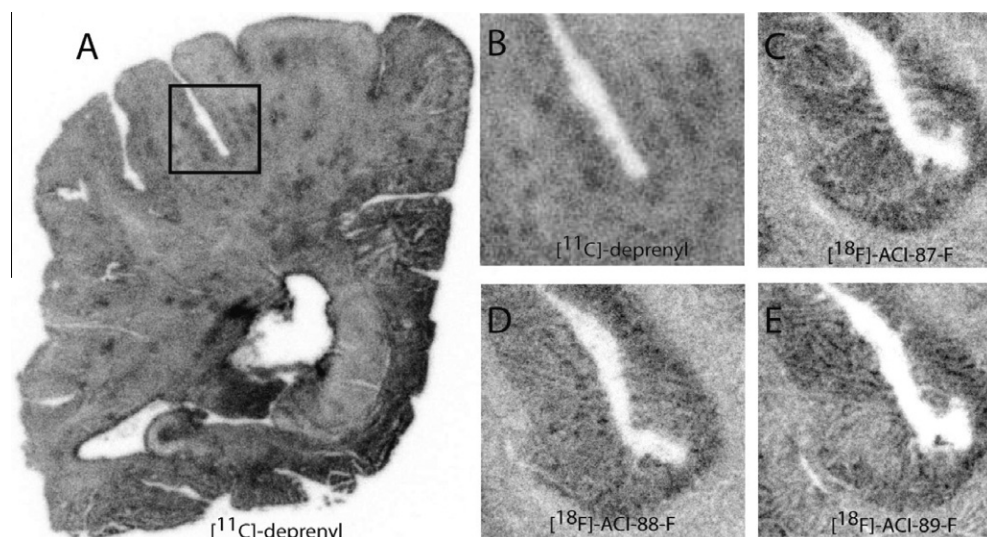

Fig. 5. [^{11}C]-L-deprenyl, [^{18}F]ACI-87-F, [^{18}F]ACI-88-F and [^{18}F]ACI-89-F autoradiography. A: [^{11}C]deprenyl autoradiography of whole hemisphere of 50 years old Alzheimer's patient. B–E: [^{11}C]deprenyl, [^{18}F]ACI-87-F, [^{18}F]ACI-88-F and [^{18}F]ACI-89-F autoradiography at higher magnification of sulcus precentralis of the same patient. The size of the square in A, and, consequently, the size of panels B–E, are 13 × 13 mm.

molecular imaging biomarkers with PET in early disease stages provides us with a non-invasive approach to visualize disease specific biochemical alterations in the human body. In the case of Alzheimer's disease the identification of specific biochemical targets in the brain, characteristic for the disease, is a key issue in order to use them as targets for molecular imaging biomarkers and, eventually, as targets for clinical diagnostic tools.

Most of the biochemical targets which are recently in the forefront of molecular imaging biomarker research in AD are partly related to neuroinflammation-specific intracellular proteins, such as TSPO in microglia and MAO-B in astrocytes, and partly to pathological protein deposits, such as defective tau proteins or $A\beta$ amyloids. The pioneering PET radioligand for amyloid imaging is [11C]PIB (Klunk et al., 2004; Lopresti et al., 2005; Price et al., 2005; Mintun et al., 2006), which has in been tested widely in the past years in AD and in other neurodegenerative diseases, including Lewy body disease (LBD) (Maetzler et al., 2009), mild cognitive impairment (MCI) (Forsberg et al., 2008; Koivunen et al., 2011), fronto-temporal dementia (FTD) (Engler et al., 2008), Parkinson's disease (Johansson et al., 2008) and amyotrophic lateral sclerosis (ALS) (Yamakawa et al., in press). Based on the accumulated evidence, a careful evaluation of the imaging capacity of [11C]PIB suggests that imaging biomarkers with shorter brain wash-out time and with lower non-specific binding in the brain, with special regard to the white matter, would be more advantegous in diagnostic amyloid imaging in the future. In order to identify more suitable amyloid PET radioligands, the search for, and testing of, novel compounds has intensified during recent years. Radiolabeled compounds with binding affinity for amyloid has been developed and tested, including [18F]AV-45 (Choi et al., 2009; Lin et al., 2010a,b; Liu et al., 2010; Yao et al., 2010), [11C]AZD2184 (Anderson et al., 2010; Johnson et al., 2009; Nyberg et al., 2009), [18F]AZD4694 (Juréus et al., 2010), [18F]BAY94-9172 (Rowe et al., 2008; O'Keefe et al., 2009).

Recently the dodekapeptide D1 (QSHYRHISPAQV) has been identified as a prospective ligand with high *ex vivo* binding affinity to beta-amyloid (Schumacher et al., 1996; Wiesehan et al., 2003; Wiesehan and Willbold, 2003), and with *in vivo* staining characteristics in transgenic AD mouse models (van Groen et al., 2008, 2009). The peptide has been radiolabeled with F18 and its radiolabeled analogues were successfully tested in post mortem human brain tissue for amyloid staining (Jahan et al., in press). The present study aimed at a detailed autoradiographic investigation of various D1 analogues, radiolabeled with 125I or 18F, in whole hemisphere human brain slices obtained from AD patients and age matched control subjects. Disease specific signs in the AD brain tissue were confirmed with immunohistochemistry as well as with complimentary autoradiographic studies using [11C]-L-deprenyl, a radioligand of activated astrocytes and up-regulated MAO-B.

The histological studies, using the amyloid stain Congo red, demonstrated the presence of amyloid in the whole hemisphere human brain slices identical with, or adjacent to, the slices used for the ARG measurements. The immunohistochemical studies using the astrocyte stain DAB confirmed in the same regions the presence of activated astrocytes which are present in and around amyloid deposits (Mrak and Griffin, 2001; Mrak, 2009). This observation was further supported by ARG studies in brain slices, adjacent to the slices used for autoradiography with the radiolabeled peptides, stained with the MAO-B radioligand [11C]-L-deprenyl. The ARG studies using both the 125I and 18F labeled peptide analogues visualized high regional radioligand uptake in those regions which were identified with the aforementioned histological, immunohistochemical and autoradiographic techniques, indicating the radioligands' s binding to amyloid in post mortem human brain tissue.

Regarding the comparison between the 125I-labeled and 18F-labeled peptides, in the AD brains the latter ones yielded better contrast between grey matter and white matter (range: 1.07–1.21 vs. 1.79–2.18, 125I and 18F, respectively). In the case of the 125I-labeled radioligands, [125I]-ACI-80 had a better grey matter: white matter contrast and the uptake differences between the two brain compartments were significant, whereas [125I]-ACI-80-F yielded lower contrast between the grey matter and white matter and the uptake differences were not significant. In the case of the 18F-labeled radioligands [18F]ACI-89-F had the highest uptake values in both grey matter and white matter 7.57 vs. 4.23 Bq/g, respectively), but at the same time the contrast between grey matter and white matter uptakes was the lowest one among the three 18F-labeled compounds (1.79). On the other hand, [18F]ACI-87-F yielded the lowest uptake values in grey and white matter (4.98 vs. 2.28 Bq/g, respectively), but the highest contrast (2.18). Finally, [18F]ACI-88-F had the medium uptake values and contrast (values: 6.46 vs. 3.12 Bq/g; contrast: 2.07). Regarding the 18F-labeled radioligands, this was the rank order not only in the case of the AD brains but also in the case of age matched control brains, wherein for each radioligands the uptake values for the grey matter components were lower than the corresponding values in AD brains. The grey matter: white matter contrast in all cases were significant. Using [3H]PIB, the grey matter: white matter binding ratios, i.e. contrast, in AD brains were around 1, whereas they were between 4 and 6 with [3H]AZD2184, the radioligand know for its most its lowest white matter uptake until today (Johnson et al., 2009).

Taken together all this evidence, the present investigations support the potential of the radiolabeled analogues of ACI-80, with special regard to [18F]ACI-89-F, as potential molecular imaging biomarkers for amyloid in the human brain. Further *in vivo* neuroimaging studies are required to explore the 18F-labeled radioligands' imaging capacity as prospective molecular imaging biomarkers of amyloid deposits in the living human brain.

Disclosure

During the process of this study, AC Immune entered into research agreement with Karolinska Institutet based on the technology described in this article. Dieter Willbold is a co-inventor of D1 and a consultant for AC Immune. All authors listed as having an AC Immune affiliation are AC Immune employees. Christian Spenger is an employee of Prodema Medical which coordinated the experiments between the different parties involved.

Acknowledgements

References

Andreasen, N., Zetterberg, H., 2008. Amyloid-related biomarkers for Alzheimer's disease. Curr. Med. Chem. 15, 766–771.

Andersson, J.D., Varnäs, K., Cselényi, Z., Gulyás, B., Wensbo, D., Finnema, S.J., Swahn, B.M., Svensson, S., Nyberg, S., Farde, L., Halldin, C., 2010. Radiosynthesis of the candidate beta-amyloid radioligand [(11)C]AZD2184: positron emission tomography examination and metabolite analysis in cynomolgus monkeys. Synapse 64, 733–741.

Banati, R.B., 2002. Visualising microglial activation in vivo. Glia 40, 206–217.

Brookmeyer, R., Johnson, E., Ziegler-Graham, K., Arrighi, H.M., 2007. Forecasting the global burden of Alzheimer's disease. Alzheimers Dement. 3, 186–191.

Brookmeyer, R., Evans, D.A., Hebert, L., Langa, K.M., Heeringa, S.G., Plassman, B.L., Kukull, W.A., 2011. National estimates of the prevalence of Alzheimer's disease in the United States. Alzheimers Dement. 7, 61–73.

Cai, L., Innis, R.B., Pike, V.W., 2007. Radioligand development for PET imaging of beta-amyloid (Abeta) – current status. Curr. Med. Chem. 14, 19–52.

Cavedo, E., Frisoni, G.B., 2011. The dynamic marker hypothesis of Alzheimer's disease and its implications for clinical imaging. Q. J. Nucl. Med. Mol. Imag. 55, 237–249.

Chen, M.K., Guilarte, T.R., 2008. Translocator protein 18 kDa (TSPO) molecular sensor of brain injury and repair. Pharmacol. Ther. 118, 1–17.

Choi, S.R., Golding, G., Zhuang, Z., Zhang, W., Lim, N., Hefti, F., Benedum, T.E., Kilbourn, M.R., Skovronsky, D., Kung, H.F., 2009. Preclinical properties of 18F-AV-45: a PET agent for Abeta plaques in the brain. J. Nucl. Med. 50, 1887–1894.

Dollé, F., Luus, C., Reynolds, A., Kassiou, M., 2009. Radiolabeled molecules for imaging the translocator protein (18 kDa) using positron emission tomography. Curr. Med. Chem. 16, 2899–2923.

Engler, H., Santillo, A.F., Wang, S.X., Lindau, M., Savitcheva, I., Nordberg, A., Lannfelt, L., Långström, B., Kilander, L., 2008. In vivo amyloid imaging with PET in frontotemporal dementia. Eur. J. Nucl. Med. Mol. Imag. 35, 100–106.

Forsberg, A., Engler, H., Almkvist, O., Blomquist, G., Hagman, G., Wall, A., Ringheim, A., Långström, B., Nordberg, A., 2008. PET imaging of amyloid deposition in patients with mild cognitive impairment. Neurobiol. Aging. 29, 1456–1465.

Fowler, J.S., Wang, G.J., Logan, J., Xie, S., Volkow, N.D., MacGregor, R.R., Schlyer, D.J., Pappas, N., Alexoff, D.L., Patlak, C., Wolf, A.P., 1995. Selective reduction of radiotracer trapping by deuterium substitution: comparison of carbon-11-L-deprenyl and carbon-11-deprenyl-D2 for MAO B mapping. J. Nucl. Med. 36, 1255–1262.

Fuller, S., Münch, G., Steele, M., 2009. Activated astrocytes: a therapeutic target in Alzheimer's disease? Expert Rev. Neurother. 9, 1585–1594.

Galimberti, D., Scarpini, E., 2011. Progress in Alzheimer's disease. J Neurol. (Epub ahead of print).

Gavish, M., Bachman, I., Shoukrun, R., Katz, Y., Veenman, L., Weisinger, G., Weizman, A., 1999. Enigma of the peripheral benzodiazepine receptor. Pharmacol. Rev. 51, 629–650.

Gulyás, B., Sóvágó, J., Sandell, J., Halldin, C., Cselényi, Z.M., Vas, Á., Kiss, B., Kárpáti, E., Farde, L., 2002. Drug distribution in man: a positron emission tomography study after oral administration of the labeled neuroprotective drug vinpocetine. Eur. J. Nucl. Med. 29, 1031–1038.

Gulyás, B., Halldin, C., Sandell, J., Swahn, C.-G., Bönöck, P., Kiss, B., Vas, Á., Cselényi, Z.M., Vas, Á., Farde, L., 2002. PET studies on the uptake and regional distribution of [^{11}C]vinpocetine in human subjects. Acta Neurol. Scand. 106, 325–332.

Gulyás, B., Makkai, B., Kása, P., Gulya, K., Bakota, L., Várszegi, S., Beliczai, Z., Andersson, J., Csiba, L., Thiele, A., Dyrks, T., Suhara, T., Suzuki, K., Higuchi, M., Halldin, C., 2009. A comparative autoradiography study in post mortem whole hemisphere human brain slices taken from Alzheimer patients and age-matched controls using two radiolabeled DAA1106 analogues with high affinity to the peripheral benzodiazepine receptor (PBR) system. Neurochem. Int. 54, 28–36.

Gulyás, B., Brockschnieder, D., Nag, S., Pavlova, E., Kása, P., Beliczai, Z., Légrádi, A., Gulya, K., Thiele, A., Dyrks, T., Halldin, C., 2010. The norepinephrine transporter (NET) radioligand (S, S)-[^{18}F]FMeNER-D2 shows significant decreases in NET density in the human brain in Alzheimer's disease: a post-mortem autoradiographic study. Neurochem. Int. 56, 789–798.

Gulyás, B., Pavlova, E., Kása, P., Gulya, K., Bakota, L., Várszegi, S., Keller, E., Horváth, M.C., Nag, S., Hermecz, I., Magyar, K., Halldin, C., 2011a. Activated MAO-B in the brain of Alzheimer patients, demonstrated by [(11)C]-l-deprenyl using whole hemisphere autoradiography. Neurochem. Int. 58, 60–68.

Gulyás, B., Vas, A., Tóth, M., Takano, A., Varrone, A., Cselényi, Z., Schain, M., Mattsson, P., Halldin, C., 2011b. Age and disease related changes in the translocator protein (TSPO) system in the human brain: positron emission tomography measurements with [(11)C]vinpocetine. Neuroimage 56, 1111–1121.

Gulyás, B., Tóth, M., Vas, A., Shchukin, E., Kostulas, K., Hillert, J., Halldin, C., 2011. Visualising neuroinflammation in post-stroke patients: a comparative PET study with the TSPO molecular imaging biomarkers [(11)C]PK11195 and [(11)C]Vinpocetine. Curr. Radiopharm. (Epub ahead of print).

Hall, H., Halldin, C., Farde, L., Sedvall, G., 1998. Whole hemisphere autoradiography of the postmortem human brain. Nucl. Med. Biol. 25, 715–719.

Hampel, H., Bürger, K., Teipel, S.J., Bokde, A.L., Zetterberg, H., Blennow, K., 2008. Core candidate neurochemical and imaging biomarkers of Alzheimer's disease. Alzheimers Dement. 4, 38–48.

Jahan, M., Nag, S., Krasikova, R., Weber, U., Muhs, A., Spenger, C., Willbold, D., Gulyás, B., Halldin, C., in press. Flourine-18 labeling of three novel D-Peptides by conjugation with N-succinimidyl-4-[F-18]fluorobenzoate and preliminary examination by post mortem whole hemisphere human brain autoradiography. Nul. Med. Biol.

Johansson, A., Engler, H., Blomquist, G., Scott, B., Wall, A., Aquilonius, S.M., Långström, B., Askmark, H., 2007. Evidence for astrocytosis in ALS demonstrated by [11C](L)-deprenyl-D2 PET. Neurol. Sci. 255, 17–22.

Johansson, A., Savitcheva, I., Forsberg, A., Engler, H., Långström, B., Nordberg, A., Askmark, H., 2008. [(11)C]-PIB imaging in patients with Parkinson's disease: preliminary results. Parkinsonism Relat Disord. 14, 345–347.

Johnson, A.E., Jeppsson, F., Sandell, J., Wensbo, D., Neelissen, J.A., Juréus, A., Ström, P., Norman, H., Farde, L., Svensson, S.P., 2009. AZD2184: a radioligand for sensitive detection of beta-amyloid deposits. J. Neurochem. 108, 1177–1786.

Johnström, P., Clark, J.C., Pickard, J.D., Davenport, A.P., 2008. Automated synthesis of the generic peptide labeling agent N-succinimidyl 4-[18F]fluorobenzoate and application to 18F-label the vasoactive transmitter urotensin-II as a ligand for positron emission tomography. Nucl. Med. Biol. 35, 725–731.

Juréus, A., Swahn, B.M., Sandell, J., Jeppsson, F., Johnson, A.E., Johnström, P., Neelissen, J.A., Sunnemark, D., Farde, L., Svensson, S.P., 2010. Characterization of

AZD4694, a novel fluorinated Abeta plaque neuroimaging PET radioligand. J. Neurochem. 114, 784–794.

Kassiou, M., Meikle, S.R., Banati, R.B., 2005. Ligands for peripheral benzodiazepine binding sites in glial cells. Brain Res. Brain Res. Rev. 48, 207–210.

Klunk, W.E., Engler, H., Nordberg, A., Wang, Y., Blomqvist, G., Holt, D.P., Bergström, M., Savitcheva, I., Huang, G.F., Estrada, S., Ausén, B., Debnath, M.L., Barletta, J., Price, J.C., Sandell, J., Lopresti, B.J., Wall, A., Koivisto, P., Antoni, G., Mathis, C.A., Långström, B., 2004. Imaging brain amyloid in Alzheimer's disease with Pittsburgh Compound-B. Ann. Neurol. 55, 306–319.

Koivunen, J., Scheinin, N., Virta, J.R., Aalto, S., Vahlberg, T., Någren, K., Helin, S., Parkkola, R., Viitanen, M., Rinne, J.O., 2011. Amyloid PET imaging in patients with mild cognitive impairment: a 2-year follow-up study. Neurology 76, 1085–1090.

Kumlien, E., Bergström, M., Lilja, A., Andersson, J., Szekeres, V., Westerberg, C.E., Westerberg, G., Antoni, G., Långström, B., 1995. Positron emission tomography with [11C]deuterium-deprenyl in temporal lobe epilepsy. Epilepsia 36, 712–721.

Lin, C.J., Huang, H.C., Jiang, Z.F., 2010a. Cu(II) interaction with amyloid-beta peptide: a review of neuroactive mechanisms in AD brains. Brain Res. Bull. 82, 235–242.

Lin, K.J., Hsu, W.C., Hsiao, I.T., Wey, S.P., Jin, L.W., Skovronsky, D., Wai, Y.Y., Chang, H.P., Lo, C.W., Yao, C.H., Yen, T.C., Kung, M.P., 2010b. Whole-body biodistribution and brain PET imaging with [18F]AV-45, a novel amyloid imaging agent – a pilot study. Nucl. Med. Biol. 37, 497–508.

Liu, Y., Zhu, L., Plössl, K., Choi, S.R., Qiao, H., Sun, X., Li, S., Zha, Z., Kung, H.F., 2010. Optimization of automated radiosynthesis of [18F]AV-45: a new PET imaging agent for Alzheimer's disease. Nucl. Med. Biol. 37, 917–925.

Lopresti, B.J., Klunk, W.E., Mathis, C.A., Hoge, J.A., Ziolko, S.K., Lu, X., Meltzer, C.C., Schimmel, K., Tsopelas, N.D., DeKosky, S.T., Price, J.C., 2005. Simplified quantification of Pittsburgh Compound B amyloid imaging PET studies: a comparative analysis. J. Nucl. Med. 46, 1959–1972.

Maetzler, W., Liepelt, I., Reimold, M., Reischl, G., Solbach, C., Becker, C., Schulte, C., Leyhe, T., Keller, S., Melms, A., Gasser, T., Berg, D., 2009. Cortical PIB binding in Lewy body disease is associated with Alzheimer-like characteristics. Neurobiol. Dis. 34, 107–112.

Mintun, M.A., Larossa, G.N., Sheline, Y.I., Dence, C.S., Lee, S.Y., Mach, R.H., Klunk, W.E., Mathis, C.A., DeKosky, S.T., Morris, J.C., 2006. [11C]PIB in a nondemented population: potential antecedent marker of Alzheimer disease. Neurology 67, 446–452.

Mrak, R.E., Griffin, W.S., 2001. The role of activated astrocytes and of the neurotrophic cytokine S100B in the pathogenesis of Alzheimer's disease. Neurobiol. Aging 22, 915–922.

Mrak, R.E., 2009. Neuropathology and the neuroinflammation idea. J. Alzheimers Dis. 18, 473–481.

Nag, S., Lehmann, L., Heinrich, T., Thiele, A., Kettschau, G., Nakao, R., Gulyás, B., Halldin, C., 2011. Synthesis of three novel fluorine-18 labeled analogues of l-deprenyl for positron emission tomography (PET) studies of monoamine oxidase B (MAO-B). J. Med. Chem. 54, 7023–7029.

Nordberg, A., 2007. Amyloid imaging in Alzheimer's disease. Curr. Opin. Neurol. 20, 398–402.

Nordberg, A., 2008. Amyloid imaging in Alzheimer's disease. Neuropsychologia 46, 1636–1641.

Nyberg, S., Jönhagen, M.E., Cselényi, Z., Halldin, C., Julin, P., Olsson, H., Freund-Levi, Y., Andersson, J., Varnäs, K., Svensson, S., Farde, L., 2009. Detection of amyloid in Alzheimer's disease with positron emission tomography using [11C]AZD2184. Eur. J. Nucl. Med. Mol. Imag. 36, 1859–1863.

O'Keefe, G.J., Saunder, T.H., Ng, S., Ackerman, U., Tochon-Danguy, H.J., Chan, J.G., Gong, S., Dyrks, T., Lindemann, S., Holl, G., Dinkelborg, L., Villemagne, V., Rowe, C.C., 2009. Radiation dosimetry of beta-amyloid tracers 11C-PiB and 18F-BAY94-9172. J. Nucl. Med. 50, 309–315.

Price, J.C., Klunk, W.E., Lopresti, B.J., Lu, X., Hoge, J.A., Ziolko, S.K., Holt, D.P., Meltzer, C.C., DeKosky, S.T., Mathis, C.A., 2005. Kinetic modeling of amyloid binding in humans using PET imaging and Pittsburgh Compound-B. J. Cereb. Blood Flow Metab. 25, 1528–1547.

Prvulovic, D., Hampel, H., 2011. Amyloid β (Aβ) and phospho-tau (p-tau) as diagnostic biomarkers in Alzheimer's disease. Clin. Chem. Lab. Med. 49, 367–374.

Rabinovici, G.D., Jagust, W.J., 2009. Amyloid imaging in aging and dementia: testing the amyloid hypothesis in vivo. Behav. Neurol. 21, 117–128.

Razifar, P., Axelsson, J., Schneider, H., Langström, B., Bengtsson, E., Bergström, M., 2006. A new application of pre-normalized principal component analysis for improvement of image quality and clinical diagnosis in human brain PET studies–clinical brain studies using [11C]-GR205171, [11C]-L-deuterium-deprenyl, [11C]-5-Hydroxy-L-Tryptophan, [11C]-L-DOPA and Pittsburgh Compound-B. NeuroImage 33, 588–598.

Reutens, D.C., 2000. Imaging monoamine oxidase B receptor mapping. Adv. Neurol. 83, 173–176.

Rodríguez, J.J., Olabarria, M., Chvatal, A., Verkhratsky, A., 2009. Astroglia in dementia and Alzheimer's disease. Cell Death Differ. 16, 378–385.

Rowe, C.C., Ackerman, U., Browne, W., Mulligan, R., Pike, K.L., O'Keefe, G., Tochon-Danguy, H., Chan, G., Berlangieri, S.U., Jones, G., Dickinson-Rowe, K.L., Kung, H.P., Zhang, W., Kung, M.P., Skovronsky, D., Dyrks, T., Holl, G., Krause, S., Friebe, M., Lehman, L., Lindemann, S., Dinkelborg, L.M., Masters, C.L., Villemagne, V.L., 2008. Imaging of amyloid beta in Alzheimer's disease with 18F-BAY94-9172, a novel PET tracer: proof of mechanism. Lancet. Neurol. 7, 129–135.

Scheinin, N.M., Scheinin, M., Rinne, J.O., 2011. Amyloid imaging as a surrogate marker in clinical trials in Alzheimer's disease. Q. J. Nucl. Med. Mol. Imag. 55, 265–279.

Schumacher, T.N., Mayr, L.M., Minor, D.L., Milhollen, M.A., Burgess, M.W., Kim, P.S., 1996. Identification of D-peptide ligands through mirror-image phage display. Science 271, 1854–1857.

Schwab, C., McGeer, P.L., 2008. Inflammatory aspects of Alzheimer disease and other neurodegenerative disorders. J. Alzheimers Dis. 13, 359–369.

Svedberg, M.M., Hall, H., Hellström-Lindahl, E., Estrada, S., Guan, Z., Nordberg, A., Långström, B., 2009. [(11)C]PIB-amyloid binding and levels of Abeta40 and Abeta42 in postmortem brain tissue from Alzheimer patients. Neurochem. Int. 54, 347–357.

Tang, G., Zeng, W.B., Yu, M.X., Kabalka, G., 2008. Facile synthesis of N-succinimidyl 4-[18F]fluorobenzoate ([18F]SFB) for protein labeling. J. Labeled Compounds Radiopharm. 51, 68–71.

van Groen, T., Wiesehan, K., Funke, S.A., Kadish, I., Nagel-Steger, L., Willbold, D., 2008. Reduction of Alzheimer's disease amyloid plaque load in transgenic mice by D3, A D-enantiomeric peptide identified by mirror image phage display. ChemMedChem 3, 1848–1852.

van Groen, T., Kadish, I., Wiesehan, K., Funke, S.A., Willbold, D., 2009. In vitro and in vivo staining characteristics of small, fluorescent, Abeta42-binding D-enantiomeric peptides in transgenic AD mouse models. ChemMedChem 4, 276–282.

Varnäs, K., Halldin, C., Hall, H., 2004. Autoradiographic distribution of serotonin transporters and receptor subtypes in human brain. Hum. Brain Mapp. 22, 246–260.

Venneti, S., Lopresti, B.J., Wiley, C.A., 2006. The peripheral benzodiazepine receptor (Translocator protein 18 kDa) in microglia: from pathology to imaging. Prog. Neurobiol. 80, 308–322.

Wang, D., Yuen, E.Y., Zhou, Y., Yan, Z., Xiang, Y.K., 2011. Amyloid beta peptide-(1–42) induces internalization and degradation of beta2 adrenergic receptors in prefrontal cortical neurons. J. Biol. Chem. 286, 31852–31863.

Wiesehan, K., Buder, K., Linke, R.P., Patt, S., Stoldt, M., Unger, E., Schmitt, B., Bucci, E., Willbold, D., 2003. Selection of D-amino-acid peptides that bind to Alzheimer's disease amyloid peptide abeta1–42 by mirror image phage display. Chembiochem 4, 748–753.

Wiesehan, K., Willbold, D., 2003. Mirror-image phage display: aiming at the mirror. Chembiochem 4, 811–815.

Wiesehan, K., Stöhr, J., Nagel-Steger, L., van Groen, T., Riesner, D., Willbold, D., 2008. Inhibition of cytotoxicity and amyloid fibril formation by a D-amino acid peptide that specifically binds to Alzheimer's disease amyloid peptide. Protein Eng. Des. Sel. 4, pp. 241–216.

Yamakawa, Y., Shimada, H., Ataka, S., Tamura, A., Masaki, H., Naka, H., Tsutada, T., Nakanishi, A., Shiomi, S., Watanabe, Y., Miki, T., in press. Two cases of dementias with motor neuron disease evaluated by Pittsburgh compound B-positron emission tomography. Neurol Sci.

Yao, C.H., Lin, K.J., Weng, C.C., Hsiao, I.T., Ting, Y.S., Yen, T.C., Jan, T.R., Skovronsky, D., Kung, M.P., Wey, S.P., 2010. GMP-compliant automated synthesis of [(18)F]AV-45 (Florbetapir F 18) for imaging beta-amyloid plaques in human brain. Appl. Radiat. Isot. 68, 2293–2297.

Yu, J.T., Wang, N.D., Ma, T., Jiang, H., Guan, J., Tan, L., 2011. Roles of β-adrenergic receptors in Alzheimer's disease: implications of novel therapeutics. Brain Res. Bull. 84, 111–117.